



Figures and figure supplements

Prefrontal cortex supports speech perception in listeners with cochlear implants

Arefeh Sherafati et al

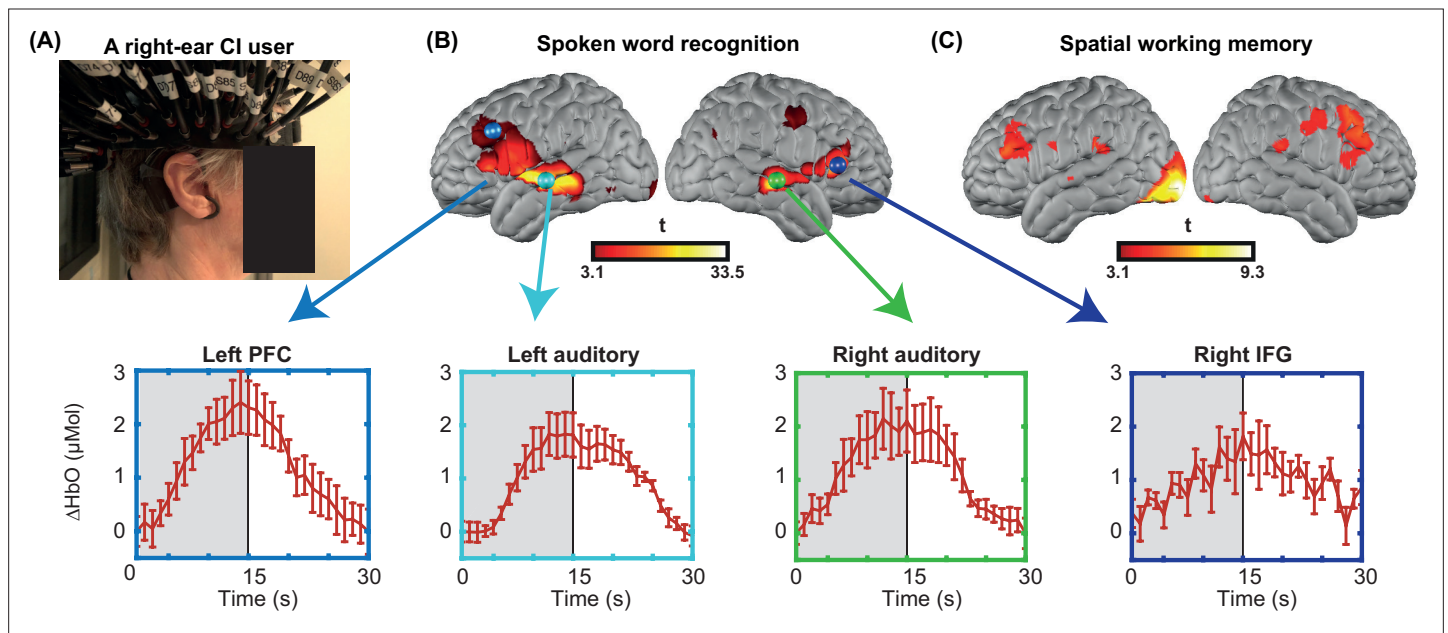


Figure 1. Single-subject data from one cochlear implant (CI) user across multiple sessions. **(A)** A CI user wearing the high-density diffuse optical tomography (HD-DOT) cap. **(B)** Response to the spoken words across six sessions (36 min of data). Hemodynamic response time-traces are plotted for peak activation values across six sessions for four brain regions. The seed colors match the plot boundaries with error bars indicating the standard error of the mean over $n=12$ runs of data. Gray shaded region indicates period during which words are presented. **(C)** Response to the spatial working memory task for the same CI user across four sessions (32 min of data).

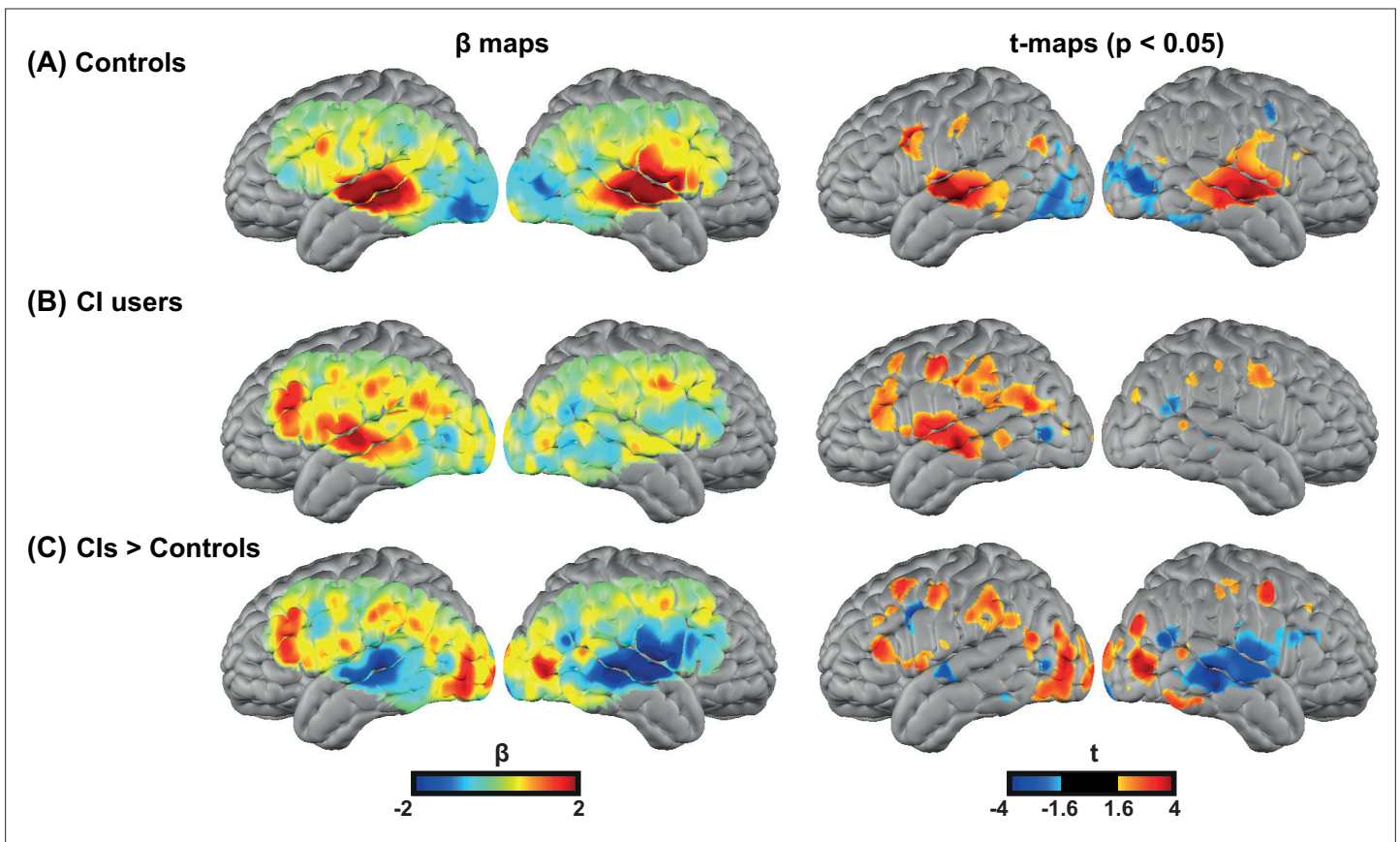


Figure 2. Spoken word recognition group maps. Response to the spoken words in **(A)** 18 controls and **(B)** 20 right ear cochlear implant (CI) users. **(C)** Differential activation in response to the spoken words task in CIs>controls highlights the group differences. The first column shows unthresholded β maps and the second column shows t-statistic maps thresholded at voxelwise $p < 0.05$ (uncorrected) for each group.

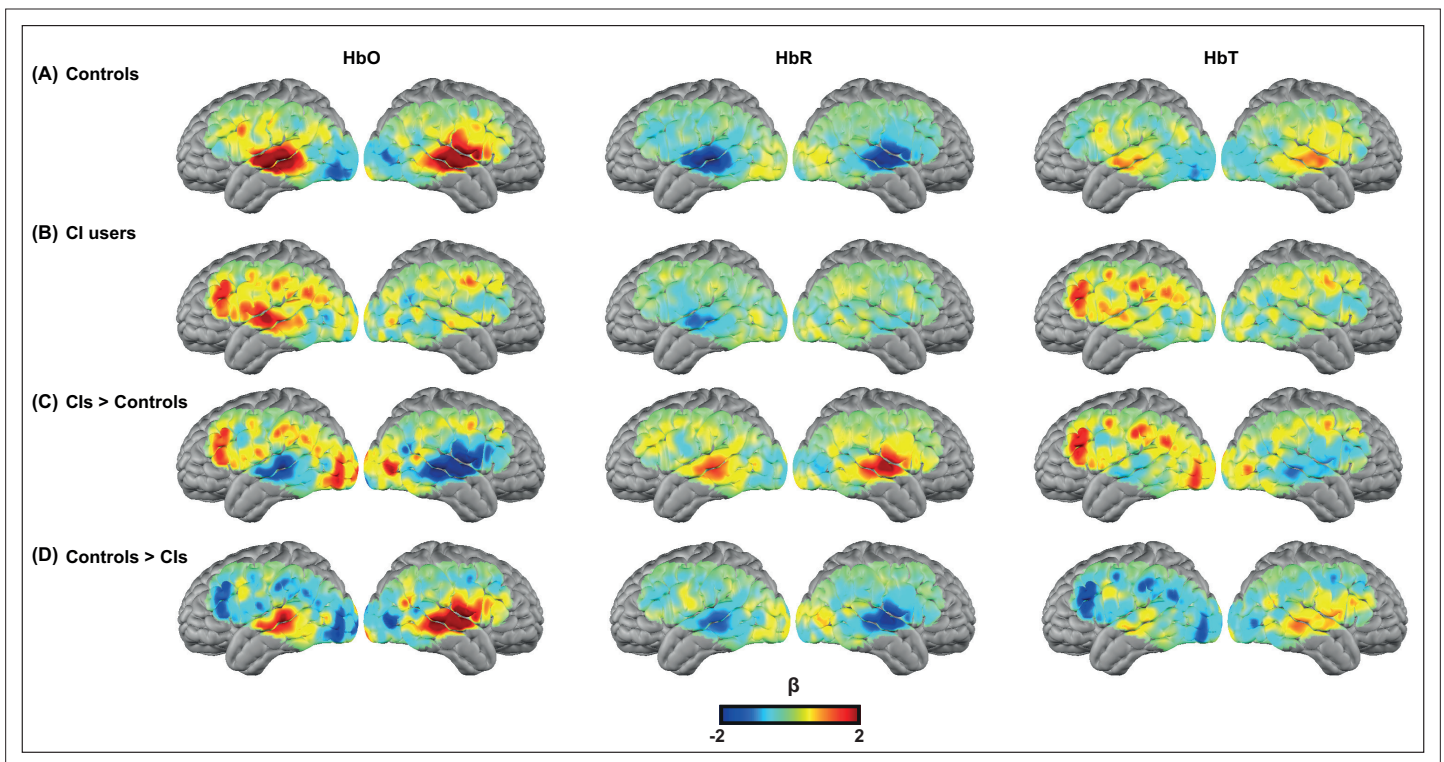


Figure 2—figure supplement 1. Group results for different hemoglobin contrasts. β maps of oxy (column 1, HbO), deoxy (column 2, HbR), and total (column 3, HbT) hemoglobin for the spoken word recognition task for (A) all controls, (B) all cochlear implant (CI) users, (C) CIs>controls, and (D) Controls>CIs. Note that the first three rows in column 1 (HbO) are identical to the results shown in **Figure 2** column 1. The redundancy is to guide the reader for side-by-side comparisons with HbR and HbT results.

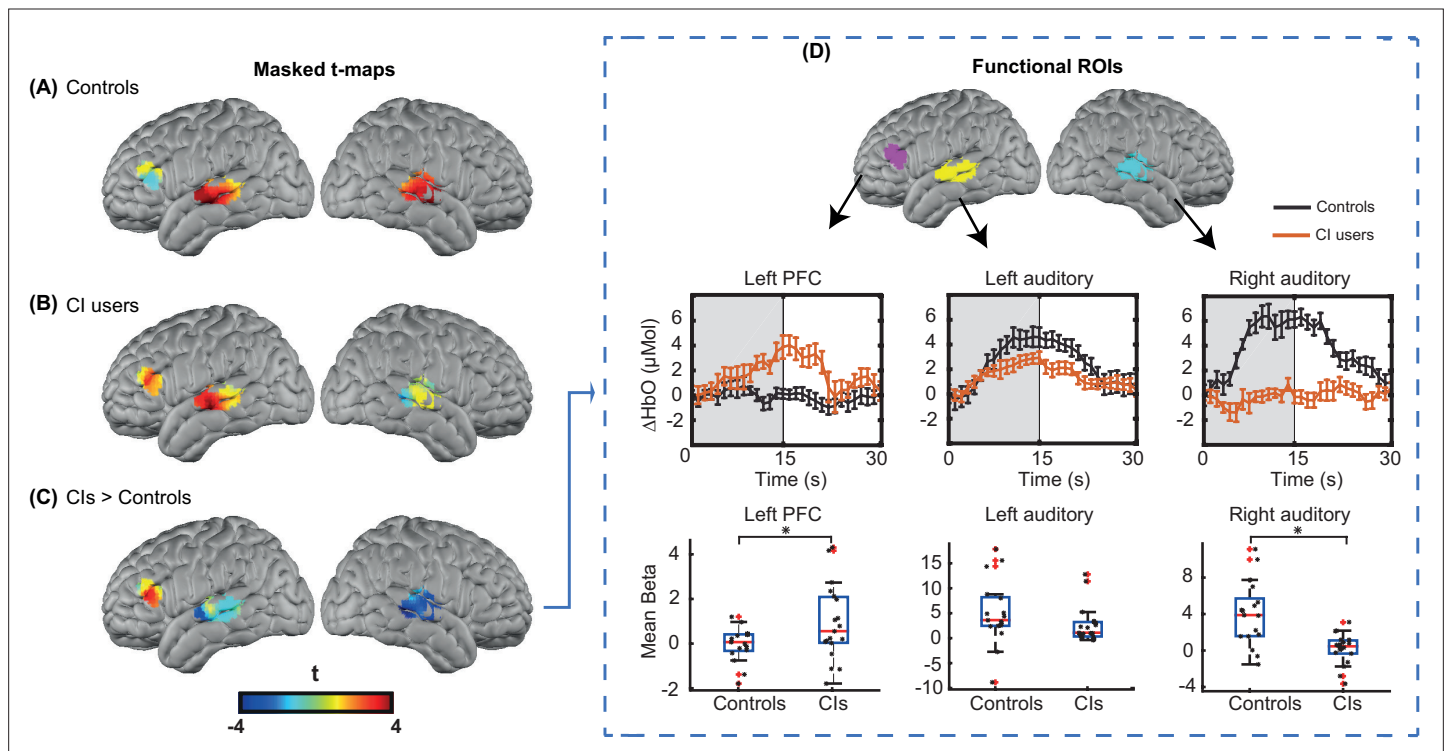


Figure 3. Region of interest (ROI)-based statistical analysis for spoken word recognition task. Unthresholded t-maps in response to the spoken words spatially masked in the three ROIs for (A) 18 controls, (B) 20 right ear cochlear implant (CI) users, and (C) CIs > controls, highlight the group differences in certain brain areas. (D) Temporal profile of the hemodynamic response in three selected ROIs (left prefrontal cortex [PFC], left auditory, and right auditory cortices). The error bars indicate the standard error of the mean over $n=20$ for CI users and $n=18$ for controls. Two-sample t-tests for mean β value in each ROI have been calculated between controls and the CI user group, confirming a significant increase in left PFC ($p=0.015$) and a significant decrease in the right auditory cortex ($p=0.0017$) in CI users (indicated by an asterisk above their corresponding box plots, corrected for multiple comparisons). The observed change in the left auditory cortex was not significant ($p=0.15$).



Figure 3—figure supplement 1. Coupling coefficients of each source and detector is shown in a flat view for all cochlear implant (CI) users included in the study. The dark red areas show the location of the signal drop for each CI user. The maximum coupling coefficient for each subject is shown above each plot.

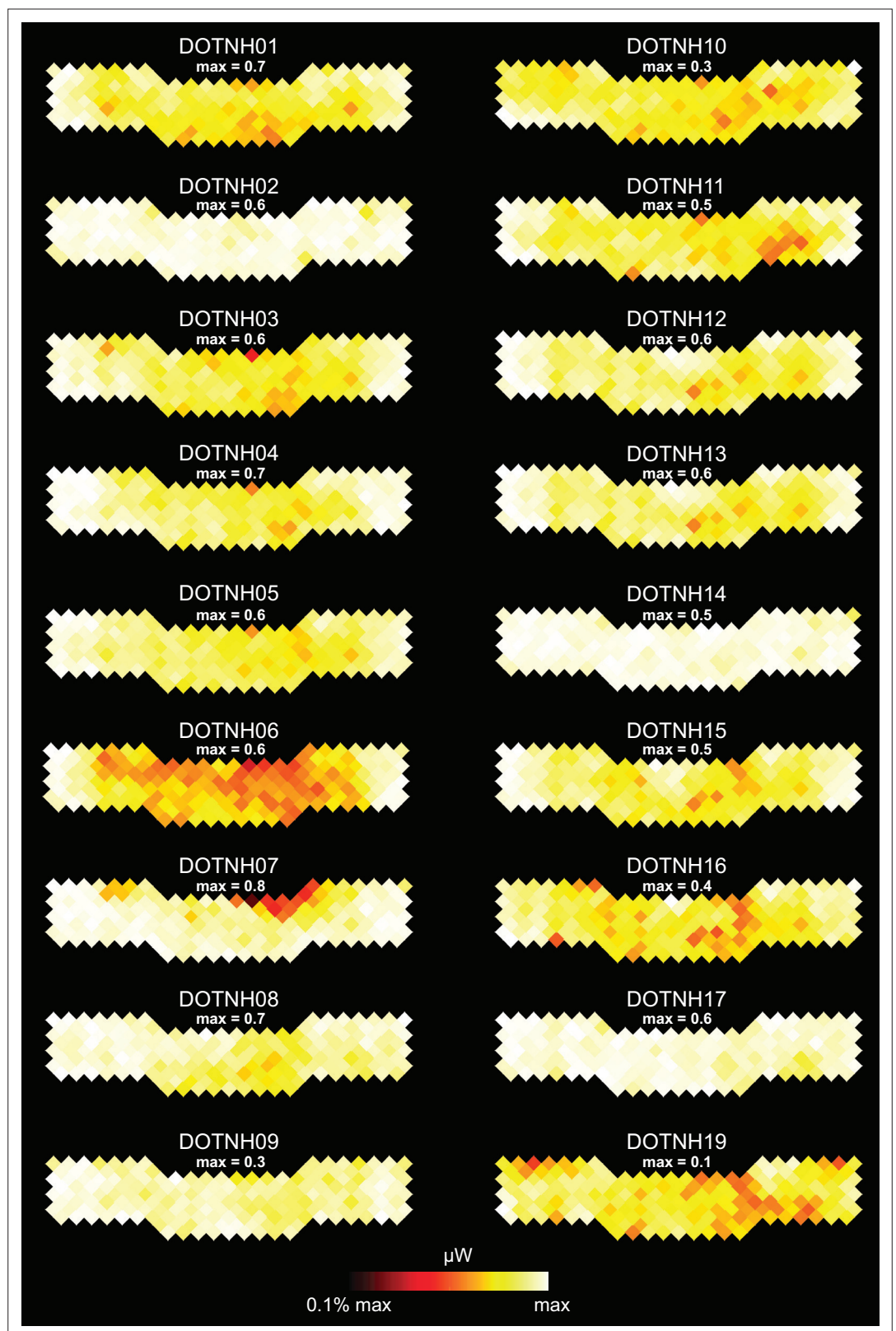


Figure 3—figure supplement 2. Coupling coefficients of each source and detector is shown in a flat view for all controls included in the study. The maximum coupling coefficient for each subject is shown above each plot.

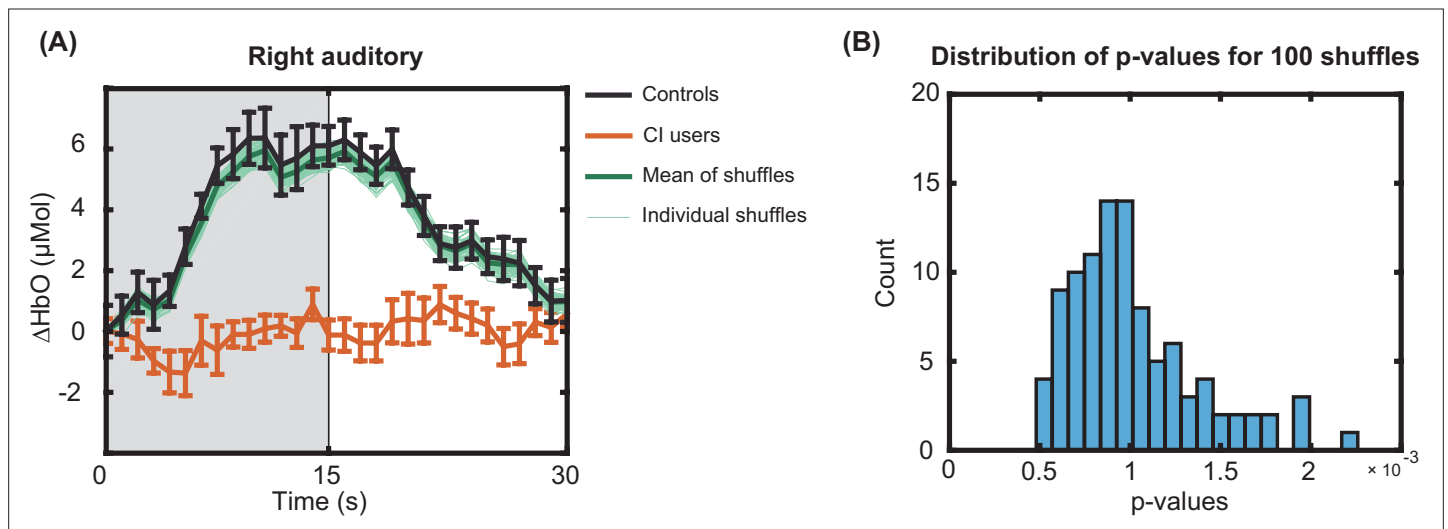


Figure 3—figure supplement 3. Effect of the simulated cochlear implant (CI) transducer in controls in the right auditory region of interest (ROI) analysis. **(A)** Replicating the ROI analysis for the right auditory cortex using 100 different shuffles of pre-processing for 18 controls by simulating the effect of the CI transducer. The error bars indicate the standard error of the mean over $n=20$ for CI users and $n=18$ for controls. **(B)** Histogram of the p-values shows statistical significance ($p < 0.016$ corrected) for all 100 shuffles across CI users and controls as found in the original pre-processing in the right auditory ROI in **Figure 3**.

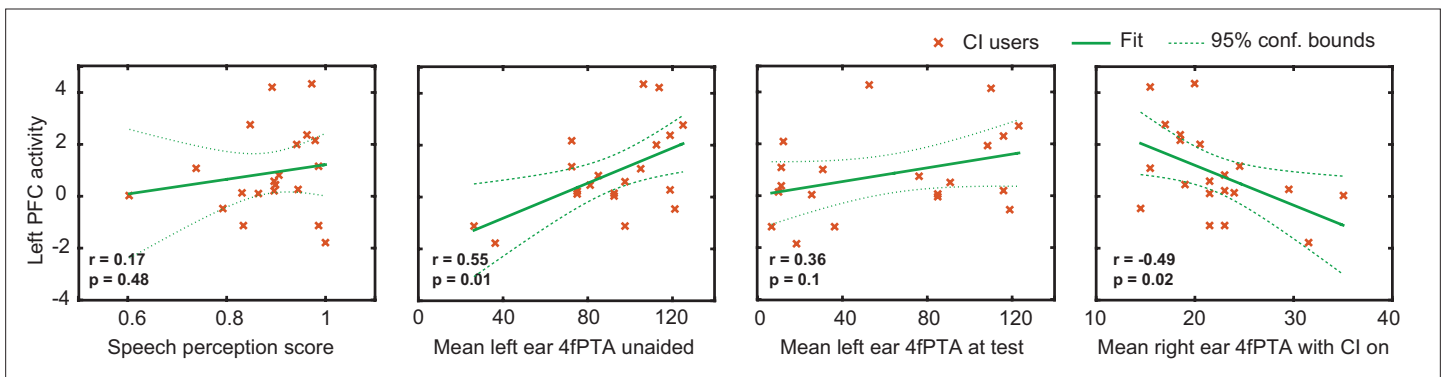


Figure 4. Relationship between the magnitude of activation in left prefrontal cortex (PFC) and behavioral scores in cochlear implant (CI) users. Plots of the Pearson correlation r between the magnitude of the mean β value in the left PFC region of interest (ROI) are shown with respect to speech perception score, left ear hearing threshold unaided, left ear hearing threshold (aided if the subject used a hearing aid), and right ear CI-aided hearing threshold. Hearing threshold was defined as four-frequency pure-tone average (4fPTA) at four frequencies, 500, 1000, 2000, and 4000 Hz.

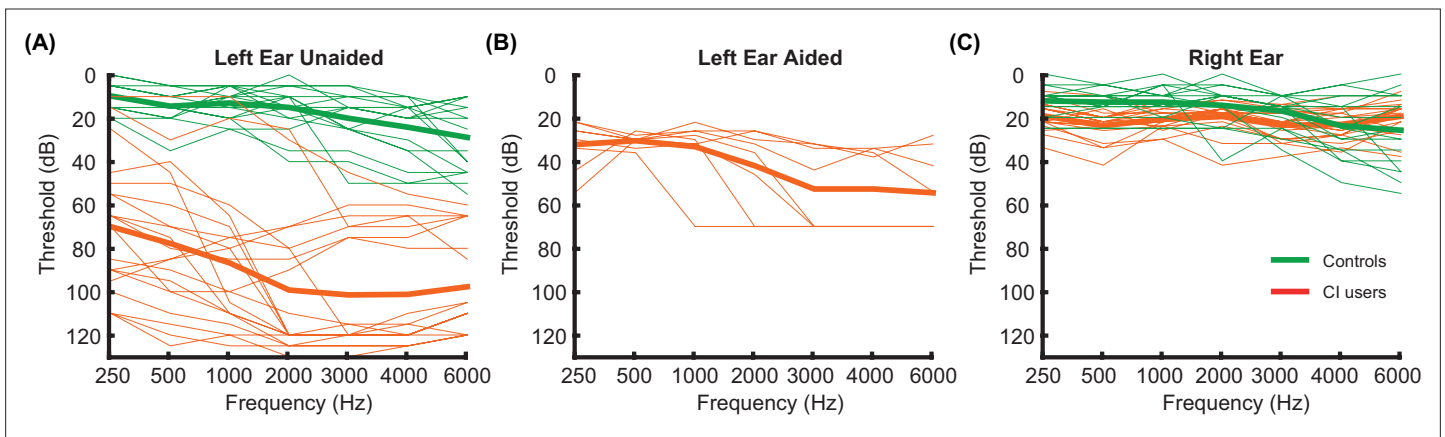


Figure 4—figure supplement 1. Audiograms for left and right ears. Individual subject (thin lines) and group mean (bold lines) hearing at 250, 500, 1000, 2000, 3000, 4000, and 6000 Hz for (A) left ear unaided, (B) left ear aided, and (C) right ear (unaided for controls and with a cochlear implant [CI] for CI users).

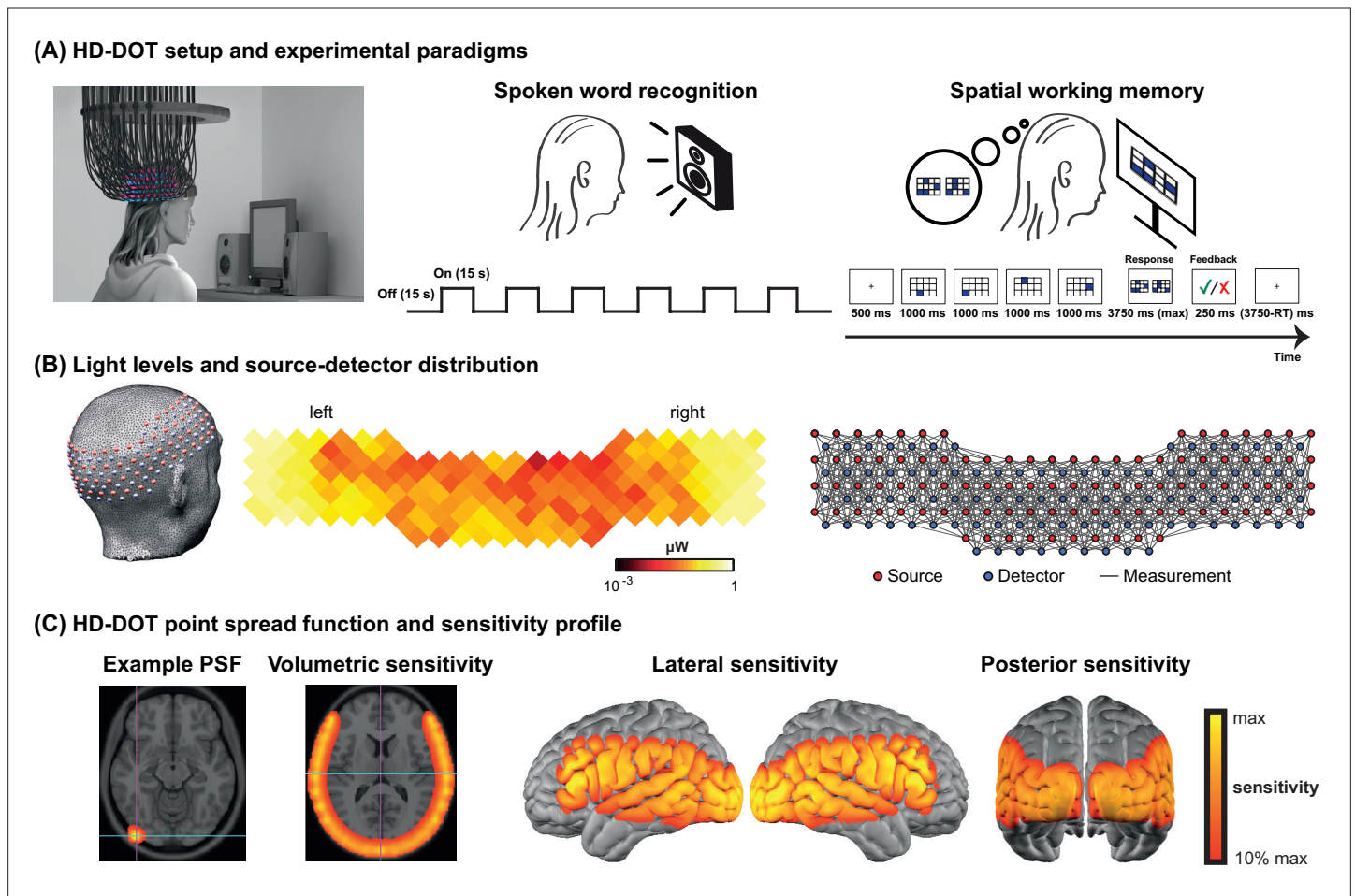


Figure 5. High-density diffuse optical tomography (HD-DOT) system and the experimental design. **(A)** Schematic of a subject wearing the HD-DOT cap along with an illustration of the task design. **(B)** Simplified illustration of the HD-DOT system (far left), regional distribution of source-detector light levels (middle), and source-detector pair measurements (~1200 pairs) as gray solid lines illustrated in a flat view of the HD-DOT cap (far right). **(C)** An example point spread function (PSF) and the HD-DOT sensitivity profile illustrated on the volume and spatially registered on the cortical view of a standard atlas in lateral and posterior views.

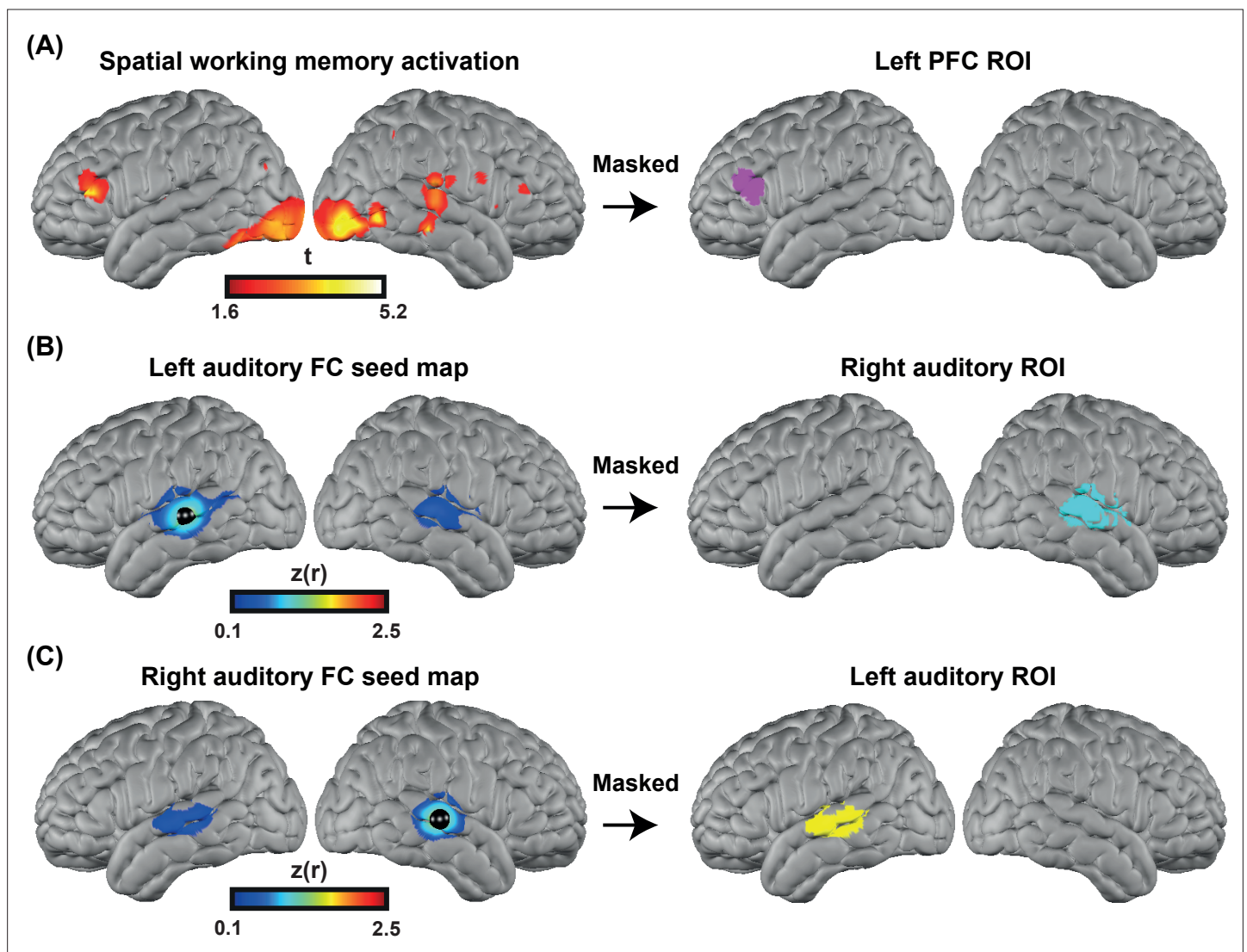
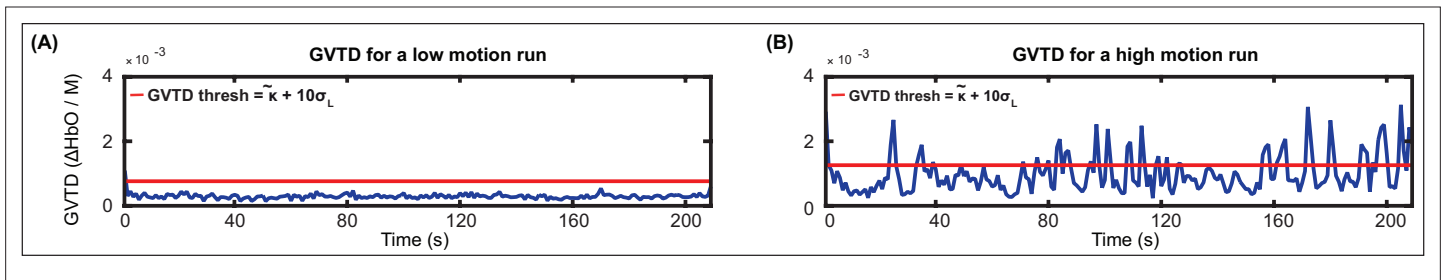
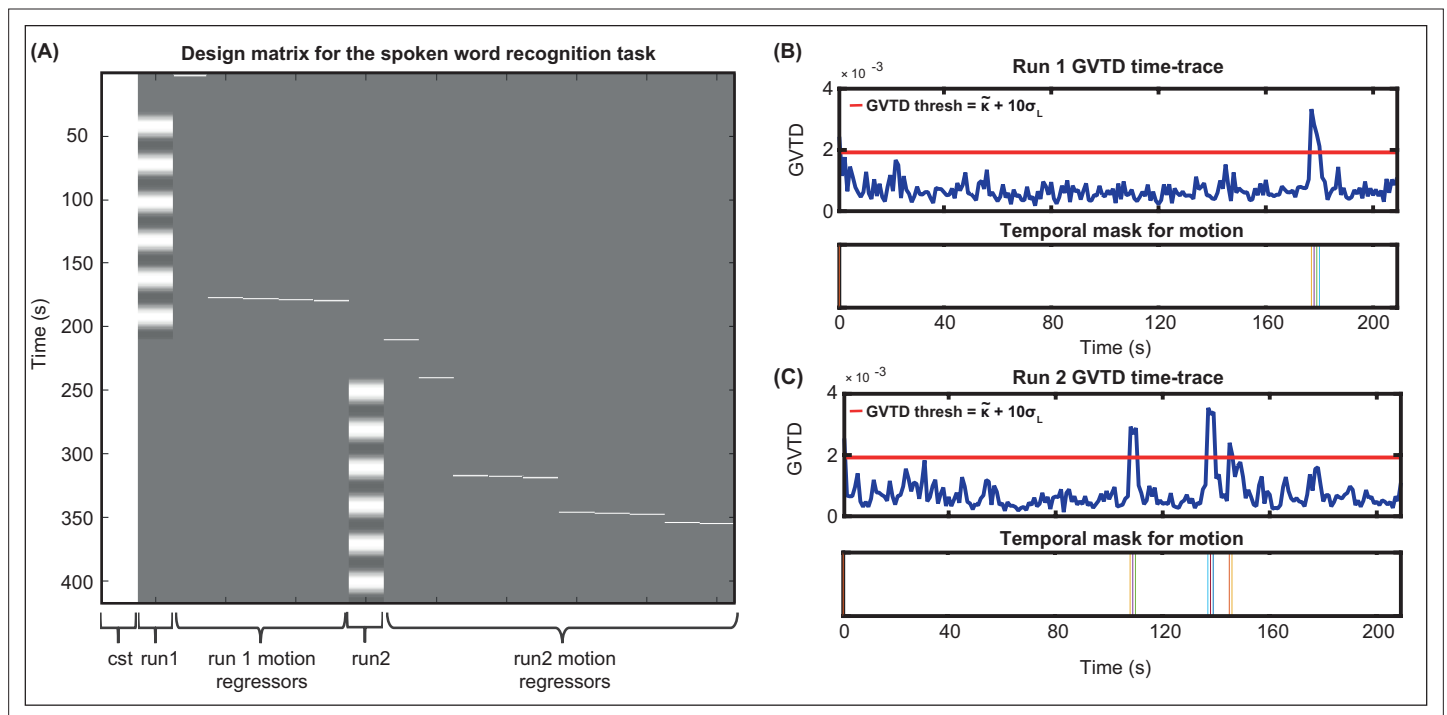


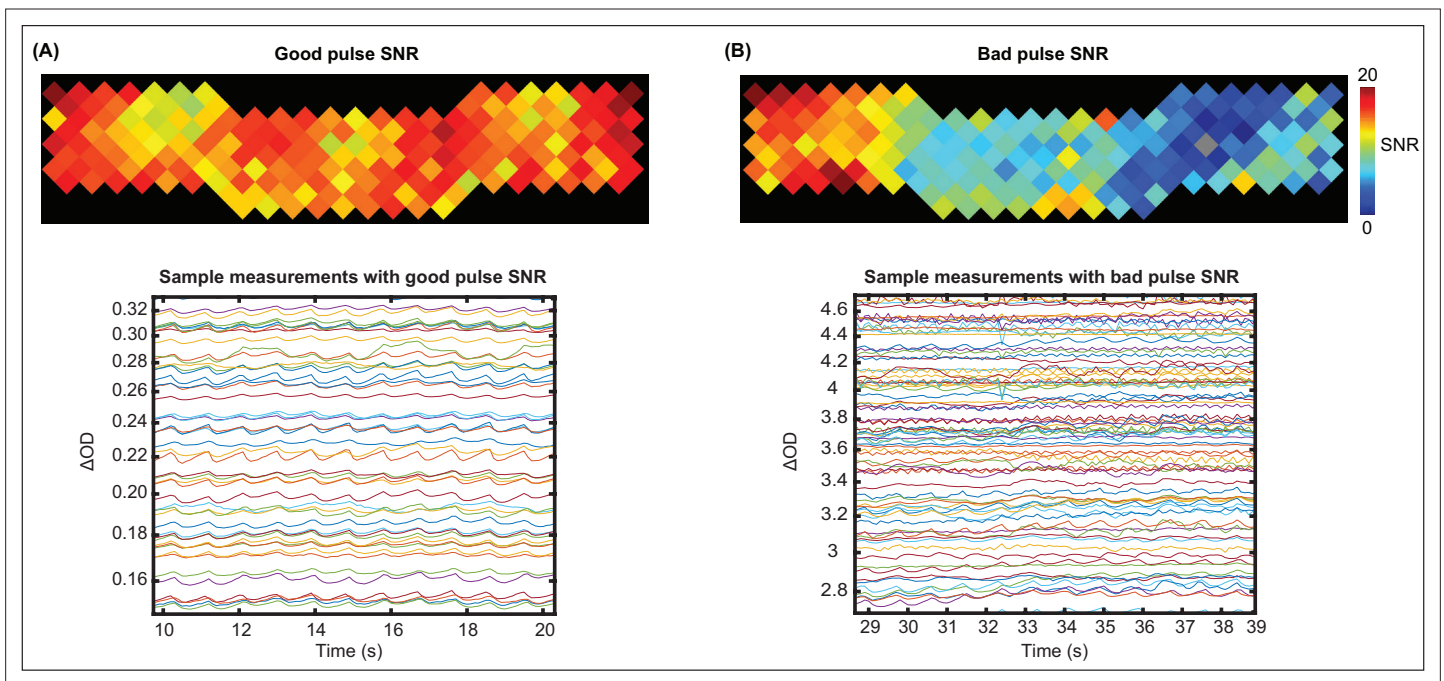
Figure 6. Defining functional regions of interest (ROIs). (A) Spatial working memory activation for five CI users and four controls over 13 sessions. The prefrontal cortex (PFC) ROI was defined as the cluster of activation in the PFC region, after $p < 0.05$ (uncorrected) voxelwise thresholding. (B) Seed-based correlation map for a seed located in the left auditory cortex (left map). Right auditory ROI defined by masking the correlation map to include only the right hemisphere (right map). (C) Seed-based correlation map for a seed located in the right auditory cortex (left map). Left auditory ROI defined by masking the correlation map to include only the left hemisphere (right map).



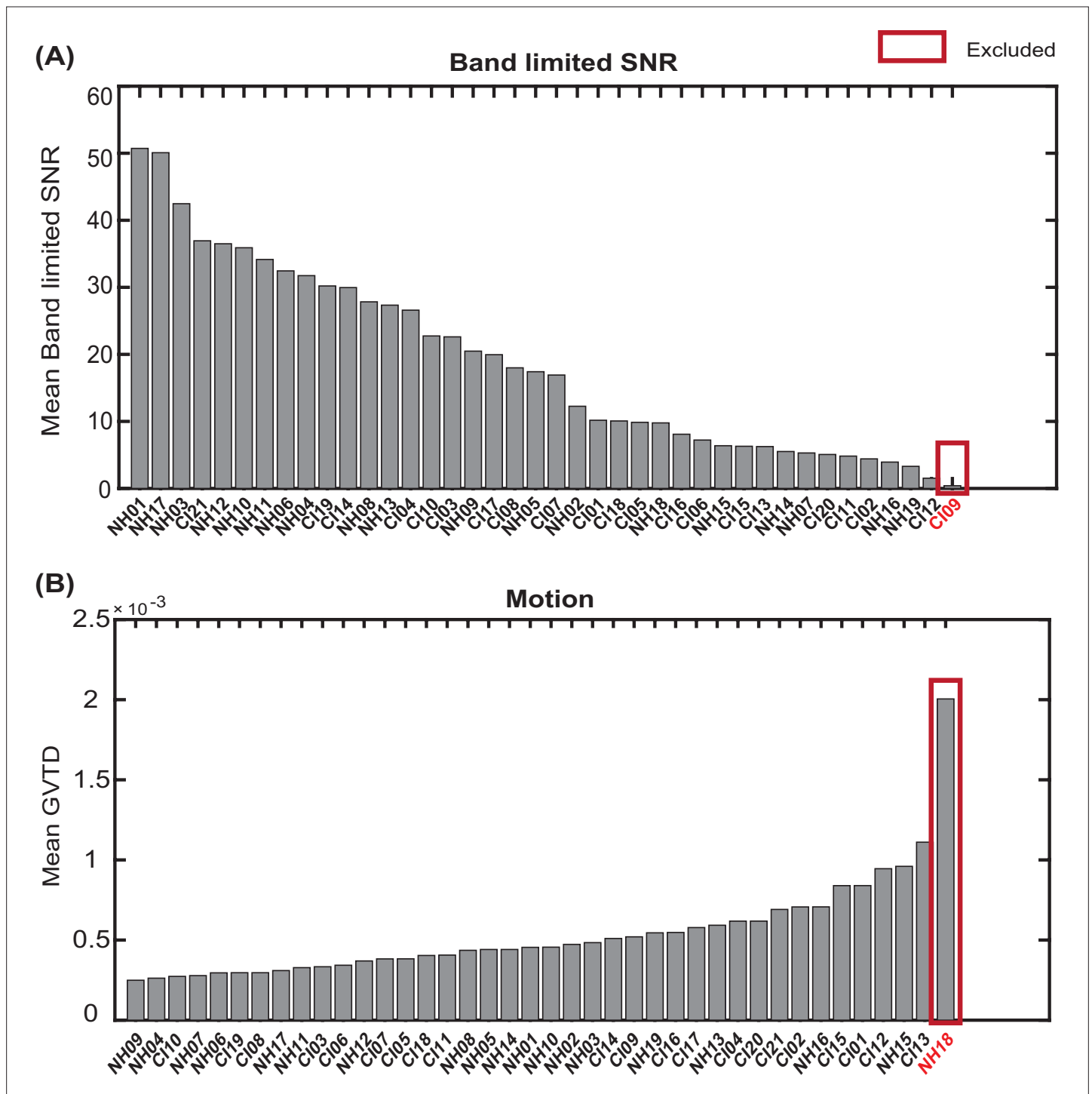
Appendix 1—figure 1. Examples of global variance of the temporal derivative (GVTD) time-traces for a low-motion and a high-motion spoken word recognition high-density diffuse optical tomography (HD-DOT) data. The red lines indicate the GVTD threshold of $\tilde{\kappa} + 10\sigma_L$ of each run.



Appendix 1—figure 2. Including motion regressors in the design matrix. **(A)** An example design matrix for the general linear model (GLM) for the spoken word recognition task, including a constant column (cst), the task times for run1, one-hot encoding columns for time-points passing the global variance of the temporal derivative (GVTD) threshold for run 1, task times for run2, and one-hot encoding columns for time-points passing the GVTD threshold for run 2. **(B)** The GVTD time-traces and the temporal masks for excluding the time-points passing the GVTD threshold are shown in **(B)** for run 1 and **(C)** for run 2.

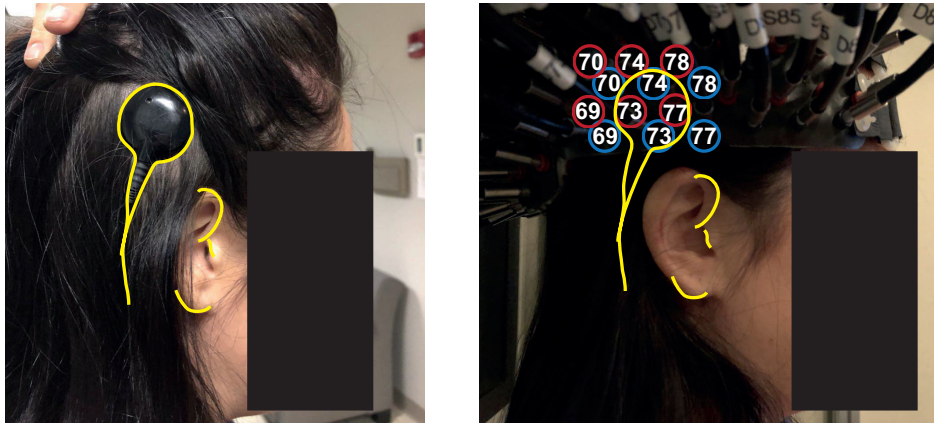


Appendix 1—figure 3. Examples of a good and a bad pulse signal-to-noise ratio (SNR) in high-density diffuse optical tomography (HD-DOT) data. Example pulse SNR plot and a selection of the measurements from the HD-DOT array for (A) a high-quality pulse SNR, and (B) a low-quality pulse SNR. Note the heartbeat frequency (~ 1 Hz) that appears as around 10 peaks in 10 s.

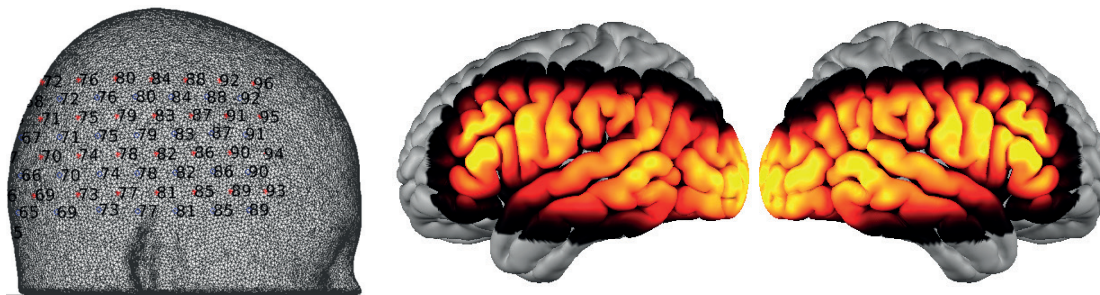


Appendix 1—figure 4. Exclusion of subjects with very low band limited signal-to-noise ratio (SNR) and very high motion levels. Sorting all subjects based on (A) mean band limited SNR value across the high-density diffuse optical tomography (HD-DOT field of view, and (B) mean global variance of the temporal derivative (GVTD) values across spoken word recognition runs. The red boxes indicate the subjects excluded based on each quality score.

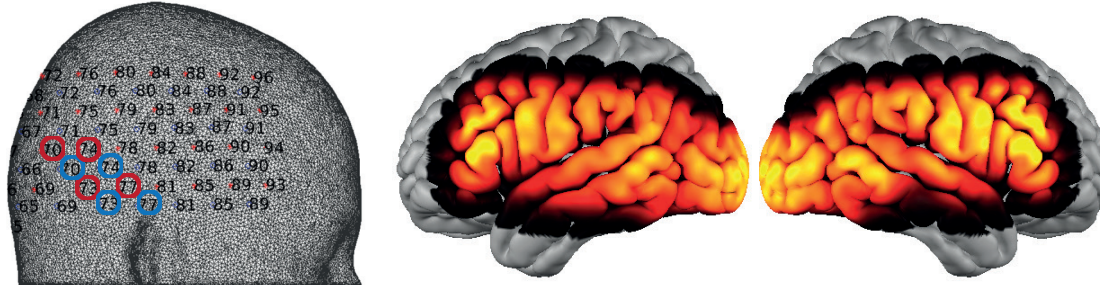
(A) Example CI user wearing the HD-DOT cap



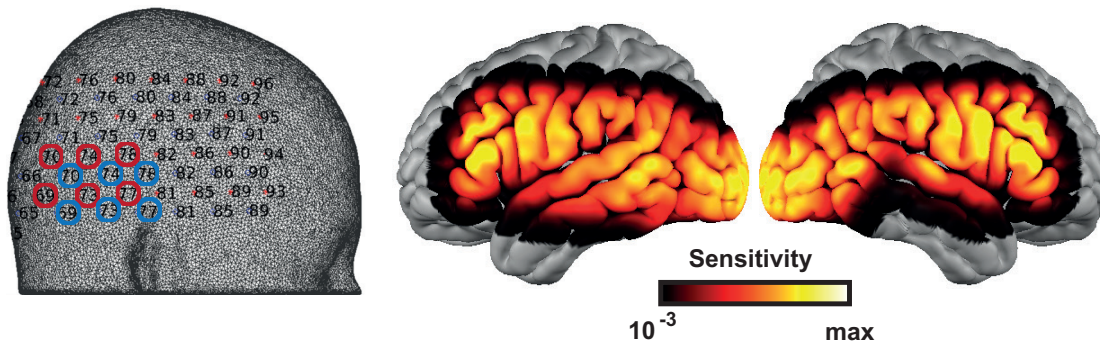
(B) Full optode array



(C) 4 sources and 4 detectors blocked



(D) 6 sources and 6 detectors blocked



Appendix 2—figure 1. Effects of the cochlear implant (CI) transducer on high-density diffuse optical tomography (HD-DOT) sensitivity. (A) A right ear CI user wearing the HD-DOT cap. The yellow contours around the CI transducer with respect to the ear fiducials illustrate the source numbers (encircled in red) and detector numbers (encircled in blue) around the transducer. (B) The left panel shows the HD-DOT source-detector grid, overlaid on the mesh used in the study for image reconstruction. The right panel shows the sensitivity of the HD-DOT cap around the cortex including all optodes. (C) The Appendix 2—figure 1 continued on next page

Appendix 2—figure 1 continued

left panel shows four sources (in red) and four detectors (in blue) excluded from the sensitivity calculation. The right panel shows the sensitivity of the HD-DOT cap excluding those sources and detectors. **(D)** The left panel shows six sources (in red) and six detectors (in blue) excluded from the sensitivity calculation. The right panel shows the sensitivity of the HD-DOT cap excluding those sources and detectors. Note that the exclusion of sources and detectors in **(C)** and **(D)** only resulted in sensitivity drop off in the inferior and middle temporal gyri.